iJRASET
International Journal For Research in Applied Science and Engineering Technology

INTERNATIONAL JOURNAL FOR RESEARCH

IN APPLIED SCIENCE & ENGINEERING TECHNOLOGY

Volume: 5 **Issue:** XI **Month of publication:** November 2017

DOI:

www.ijraset.com

Call: 08813907089 | E-mail ID: ijraset@gmail.com

International Journal for Research in Applied Science & Engineering Technology (IJRASET)
ISSN: 2321-9653; IC Value: 45.98; SJ Impact Factor:6.887
Volume 5 Issue XI November 2017- Available at www.ijraset.com

Vibration Behavior of FG-CNT Reinforced Composite Plates Subjected To Mechanical Loading

Naga chaitanya binkam[1], Dr. J. Suresh kumar[1].
[1]*Department of Mechanical Engineering, JNTUH College of Engineering, J.N.T. University, Hyderabad*

Abstract: ***This research aims at studying the free vibration analysis of CNT reinforced functionally graded composite rectangular plate using higher order shear deformation theory. The equations of motion of the structural system are derived using the Hamilton's principle. The vibration characteristics of the model in the closed form are obtained by using Navier's method for different boundary conditions. The natural frequencies and vibration mode shapes of FG-CNT reinforced composite rectangular plate subjected to transverse loads with different boundary conditions are presented for different aspect ratios by using eigen value method. The present results are compared with the solutions of the material with different reinforcement available in the literature. It can be concluded that the proposed theory is accurate and efficient in predicting the vibration behaviour of FG-CNT plates. A computer program in C is developed for determining fundamental frequencies.***
Key words: Al-CNT, FG-CNT Reinforced Composite Plates, Effective Material Properties, HSDT, Navier's Method.

I. INTRODUCTION

Functionally graded materials (FGMs) are multifunctional composites involving spatially varying volume fraction of constituent materials, thus providing a graded microstructure and macro-properties. CNT is an effective reinforcement material in the case of composite material developments, owing to its good physical and chemical properties.

Guided by the concept of functionally graded (FG) materials, a class of new emerging composite materials, the FG-CNT reinforced composite, has been proposed making use of CNTs as the reinforcements in a functionally graded pattern. Using a powder metallurgy fabrication process, carbon-nano tube-reinforced composites (CNTRCs) may be achieved with a non-uniform distribution of CNTs through the media. This type of reinforced composite media is known as functionally graded carbon-nanotube-reinforced composite (FG-CNTRC). This new type of FG-CNT reinforced composite will need further research so as to find out its mechanical properties.

The advantages of FG-CNT include multi-functionality, ability to withstand at high pressures and in harsh environments, resistant to wear and tear and ability to remove stress concentrations. Using FG-CNT, intricate shapes can be easily produced and it has Cost-effective manufacturing processes.

A number of investigations have been carried out using CNT as reinforcement in different materials, namely polymer, ceramic and metals. The majority of the research has been carried out on reinforcement of polymers by CNT. This can be attributed primarily to the relative ease of polymer processing, which often does not require high temperatures for consolidation as needed for metals and ceramic matrixes. Aluminum and its alloys, being the most abundantly used non-ferrous structural materials, were the first choice for reinforcement with carbon nanotubes. The first publication on metal-CNT system was on Al-CNT in 1998 [1]. The powder metallurgy route has been used extensively due to ease of dispersing the CNTs within the aluminum matrix. A secondary consolidation by deformation processing is advantageous in obtaining higher densities and improved CNT distribution. The composite containing 5 vol.% CNT was found to have a tensile strength 128% higher than the unreinforced material[2]. Ball milling has been used extensively to disperse the CNTs in the Al powder. Depending on the degree of dispersion, different studies reported different degrees of strengthening. Aluminum 4.5 vol.% CNT composite prepared by hot rolling of ball milled powders was shown to have a tensile yield strength of 620 MPa and fracture toughness of 61 MPa.mm which are, respectively, 15 and 7 times more than that for aluminum [3]. Plasma sprayed aluminium composite coatings made by blended powder have been shown to improve the hardness by 72%, elastic modulus by 78%, marginal improvement in tensile strength, and 46% decrease in ductility with 10 wt.%CNT addition [4]. Sintering at 673 K for 72 h of the plasma sprayed Al-10 wt.% CNT coating has been reported to further increase the elastic modulus of the composite coating by 80%, which has been attributed to reduction in porosity and residual stress [5]. Al-12 vol.% CNT composite produced by plasma spraying of spray-dried powders shows 40% increase in the elastic modulus[3].CNT addition results in an increase in the elastic recovery[3]. Al-1 vol.% CNT prepared by hot extrusion of SPS compacts have displayed tensile strengths upto four times (198 MPa) of aluminum (52 MPa)[6]. Strengthening has been observed irrespective of the formation of Al[7]. Significant strengthening has been achieved in samples produced by hot extrusion technique

because the technique can produce high densities and can lead to breakdown of CNT clusters[8].These results show that homogeneous distribution of CNTs, strong bonding with the matrix, and high density are the key factors to control the mechanical properties of the aluminum-CNT composites.

In this paper an attempt is made to study the vibration characteristics of Al-CNT where CNT is functionally graded(discrete). There were many studies of vibration behaviour on various materials using higher order theory. This is the first study where the vibration characteristics are studied for aluminium with functionally graded CNT.

FG-CNTs have wide applications in aerospace structures to withstand aero-thermal loads [9]. They are used as a reactor shield in nuclear reactors to reduce chemical corrosion and thermal stress and also as TBCs in combustion chambers. It is used in manufacturing the components of propulsion system, submarines, etc and for cutting tools.

The buckling, vibration, linear and nonlinear bending behaviours of FG-CNT reinforced composite structures have attracted much attention from researchers [10]. Using HSDT theory, L.W. Zhang et al.[11] studied the vibration analysis of FG-CNT reinforced composite plates subjected to in-plane loads based on State-space Levy method.

B. Sidda Redddy, J. Suresh Kumar, C. Eswara Reddy and K. Vijaya Kumar Reddy[12] investigated Free
Vibration Behaviour of Functionally Graded Plates Using Higher-Order Shear Deformation Theory. In
this paper the aluminium reinforced with zirconium is taken and vibration behaviour for different aspect ratios are determined and compared with the exact solution.

Mohammad Rahim Nami et al.[13] investigated the free vibration of thick functionally graded carbon nanotube-reinforced rectangular composite plates based on three dimensional elasticity theory via differential quadrature method. Based on the first-order shear deformation plate theory, Zhu et al.[14] carried out bending and free vibration analyses of thin-to-moderately thick FG composite plates reinforced by single-walled carbon nano-tubes. Results revealed the influences of the volume fractions of CNT and the edge -to- thickness ratios on the bending responses, natural frequencies and mode shapes of FG-CNTRC plates. A first known free vibration characteristics of functionally graded nano-composite triangular plates reinforced by single-walled carbon nanotubes (SWCNTs) is presented by L.W. Zhang et al.[15]. They studied the free vibration analysis of functionally graded carbon nanotube reinforced composite triangular plates using the FSDT and element-free IMLS-Ritz method.

T. Kant and K. Swaminathan [16] presented the analytical formulations and solutions to the natural frequency analysis of simply supported composite and sandwich plates using higher order shear deformation theory. The equations are formulated using Hamilton's principle and are solved by the Taylor's series of Navier's solution.

Most of the above discussed theories do not account for transverse shear stresses on the top and bottom surfaces of the plate. This must be considered while modeling of the FG-CNT Plates, because of the transverse shear stresses and strains are not zero, when the FG-CNT Plates used in aerospace structures that are subjected to transverse load/pressure

The present paper deals with the analytical formulations and solutions for the vibration analysis of FG-CNT reinforced composite plate using higher order shear deformation theory (HSDT) without enforcing zero transverse shear stress on the top and bottom surfaces of the plate. In this paper an attempt has been made to study the vibration characteristics of Aluminium reinforced with various volume fractions of CNT. The theoretical model presented herein incorporates the transverse extensibility which accounts for the transverse effects. Thus a shear correction factor is not required. The plate material is graded through the thickness direction. The plate's governing equations and its boundary conditions are derived by employing the principle of virtual work. Solutions are obtained for FG-CNT reinforced composite plate in closed-form using Navier's technique and solving the Eigen value equation. The present results are compared with the solutions of Al with ZrO_2 as reinforcement available in the literature to verify the accuracy of the proposed theory in predicting the natural frequencies of FG-CNT reinforced composite plate. The effects of side-to-thickness ratios and volume fraction exponent on the natural frequencies are studied after establishing the accuracy of the present results for FG-CNT reinforced composite plate.

II. THEORETICAL FORMULATION

In formulating the higher-order shear deformation theory, FG-CNT reinforced composite plates with two different distributions of CNT are considered. The length, width and thickness of the FG-CNT reinforced composite plate are a, b and h respectively.FG-CNT reinforced composite plates with these CNT configurations are displayed in Figure 1. One is uniform distribution of CNT denoted by UD and other is FGX for which both the top and bottom surfaces of the plate are CNT-rich.

ISSN: 2321-9653; IC Value: 45.98; SJ Impact Factor:6.887
Volume 5 Issue XI November 2017- Available at www.ijraset.com

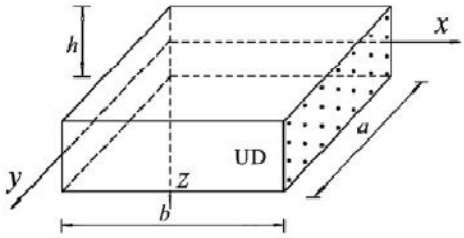

Figure 2.1 UD distribution of CNT in FG CNT plate.

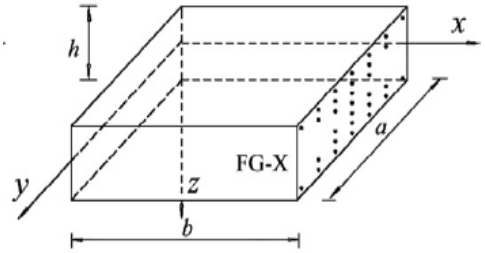

Figure 2.2 FG X distribution of CNT in FG CNT plate.

The voume fractions of the two distribution types are expressed as follows:

$V_{CNT}(z) = V^*_{CNT}$, (UD)

... (1)

$V_{CNT}(z) = \frac{4|z|}{h} V^*_{CNT}$, (FGX)

Where,

$$V^*_{CNT} = \frac{m_{CNT}}{m_{CNT} + (\rho^{CNT}/\rho^m) - (\rho^{CNT}/\rho^m)m_{CNT}}$$

in which m_{CNT} is the mass fraction of the CNTs, and ρ^m and ρ^{CNT} are densities of the matrix and CNTs.

The effective Young's module and Poisson's ratio along the thickness are calculated by:

$E_{11} = \eta_1 V_{CNT}(z) E^{CNT}_{11} + V_m(z) E^m$

$\frac{\eta_2}{E_{22}} = \frac{V_{CNT}(z)}{E^{CNT}_{22}} + \frac{V_m(z)}{E^m}$

$\frac{\eta_3}{G_{12}} = \frac{V_{CNT}(z)}{G^{CNT}_{12}} + \frac{V_m(z)}{G^m}$

$\upsilon_{12} = V^*_{CNT}\upsilon^{CNT}_{12} + V_m\upsilon^m$

$\upsilon_{21} = \upsilon_{12}E_{22}/E_{11}$ ....(2)

where E^{CNT}_{11} , E^{CNT}_{22} and G^{CNT}_{12} are the elastic and shear moduli of the transversely isotropic CNT. E^m and G^m are the corresponding properties of the isotropic matrix. CNT efficiency parameters η_1 , η_2 *and* η_3 are introduced to account for load transfer between the CNT and polymeric phases as the load transfer between the CNT and matrix is less than perfect. V_{CNT} *and* V_m are the volume fractions of the CNT and matrix, and their sum must be equal to 1, that is $V_{CNT} + V_m = 1$.

A. Displacement Model

In order to approximate 3D-elasticity plate problem to a 2D one, the displacement components u (x, y, z), v (x, y, z) and w (x, y, z) at any point in the plate are expanded in terms of the thickness coordinate. The elasticity solution demonstrates that the transverse shear stress varies parabolic ally through the plate thickness. This demands the use of a displacement field, in which the in-plane displacements are expanded as cubic functions of the thickness coordinate. The displacement field which assumes w (x, y, z) constant throgh the plate thickness thus setting $\varepsilon_z = 0$ is expressed as:

$$u(x,y,z) = u_o(x,y) + z\theta_x(x,y) + z^2 u_o^*(x,y) + z^3\theta_x^*(x,y)$$
$$v(x,y,z) = v_o(x,y) + z\theta_y(x,y) + z^2 v_o^*(x,y) + z^3\theta_y^*(x,y)$$
$$w(x,y,z) = w_o(x,y) \qquad ...(3)$$

where u_0, v_0, w_0 denote the mid-plane displacements of a point (x, y) and θ_x, θ_y are the rotations of the normal to the mid-plane about y and x axes, respectively. The parameters u_0^*, v_o^*, θ_x^*, $\theta_y^*$are the corresponding higher-order deformation terms.

By substituting displacement relations of Eq. (3) in to strain displacement equations of the classical theory of elasticity the following relations are obtained:

$$\varepsilon_x = \varepsilon_{xo} + zk_x + z^2\varepsilon_{xo}^* + z^3 k_x^*$$
$$\varepsilon_y = \varepsilon_{yo} + zk_y + z^2\varepsilon_{yo}^* + z^3 k_y^*$$
$$\varepsilon_z = 0$$
$$\gamma_{xy} = \varepsilon_{xyo} + zk_{xy} + z^2\varepsilon_{xyo}^* + z^3 k_{xy}^*$$
$$\gamma_{yz} = \phi_y + z\varepsilon_{yzo} + z^2\phi_y^*$$
$$\gamma_{xz} = \phi_x + z\varepsilon_{xzo} + z^2\phi_x^* \qquad ...(4)$$

where,

$$\varepsilon_{xo} = \frac{\partial uo}{\partial x},\ \varepsilon_{yo} = \frac{\partial vo}{\partial y},\ \varepsilon_{xyo} = \frac{\partial uo}{\partial y} + \frac{\partial v_o}{\partial x}$$
$$k_x = \frac{\partial \theta_x}{\partial x},\ k_y = \frac{\partial \theta_y}{\partial y},\ k_{xy} = \frac{\partial \theta_x}{\partial y} + \frac{\partial \theta_y}{\partial x}$$
$$k_x^* = \frac{\partial \theta_x^*}{\partial x},\ k_y^* = \frac{\partial \theta_y^*}{\partial y},\ k_{xy}^* = \frac{\partial \theta_x^*}{\partial y} + \frac{\partial \theta_y^*}{\partial x}$$

$$\varepsilon_{xo}^* = \frac{\partial u_o^*}{\partial x},\ \varepsilon_{yo}^* = \frac{\partial v_o^*}{\partial y}, \varepsilon_{xyo}^* = \frac{\partial u_o^*}{\partial y} + \frac{\partial v_o^*}{\partial x},$$
$$\phi_y = \theta_y + \frac{\partial w_o}{\partial y},\ \phi_x = \theta_x + \frac{\partial w_o}{\partial x},$$
$$\varepsilon_{yzo} = 2v_o^*, \varepsilon_{xzo} = 2u_o^*,\ \phi_y^* = 3\theta_y^*,\ \phi_x^* = 3\theta_x^*$$

B. Elastic Stress-Strain Relations

Since $\varepsilon_z = 0$, the transverse normal stressσ_z, although not zero identically, does not appear in the virtual work statement and hence in the equations of motion. Consequently, it amounts to neglecting the transverse normal stress. Thus we have, in theory, a case of plane stress [17]. For an FG-CNT rein forced composite laminate, the plane stress reduced elastic constants and the transformed plane stress reduced elastic constants will be same i.e., $C_{ij} = Q_{ij}$. The constitutive relations for FG-CNT materials can be written as:

$$\begin{Bmatrix} \sigma_x \\ \sigma_y \\ \tau_{xy} \end{Bmatrix} = \begin{bmatrix} Q_{11} & Q_{12} & 0 \\ Q_{12} & Q_{22} & 0 \\ 0 & 0 & Q_{33} \end{bmatrix} \begin{Bmatrix} \varepsilon_x \\ \varepsilon_y \\ \gamma_{xy} \end{Bmatrix}$$

$$\begin{Bmatrix}\tau_{yz}\\ \tau_{xz}\end{Bmatrix} = \begin{bmatrix}Q_{44} & 0\\ 0 & Q_{55}\end{bmatrix}\begin{Bmatrix}\gamma_{yz}\\ \gamma_{xz}\end{Bmatrix} \quad ..(5)$$

where,

$\sigma_x, \sigma_y, \tau_{xy}, \tau_{yz}, \tau_{xz}$ are the stresses and $\varepsilon_x, \varepsilon_y, \gamma_{xy}, \gamma_{yz}, \gamma_{xz}$ are the strains with respect to the axes. Q_{ij} are the plane stress reduced elastic constants in the plate axes that vary through the plate thickness and are given by:

$$Q_{11} = \frac{E_{11}}{(1-\upsilon_{12}\upsilon_{21})}, \quad Q_{22} = \frac{E_{22}}{(1-\upsilon_{12}\upsilon_{21})}, Q_{33} = G_{12},$$

$$Q_{12} = \frac{\upsilon_{21}E_{11}}{(1-\upsilon_{12}\upsilon_{21})}, \quad Q_{44} = G_{23}, Q_{55} = G_{13}$$

Where,

E_{ii} = Young's modulus of elasticity in the i direction.

υ_{ij} = Poisson's ratios that give strain in the j direction due to stress in the i direction.

G_{ij} = shear moduli , and these are computed using Eq. (2).

C. Governing Equations of Motion

The energy principle states that the work done by actual forces in moving through virtual displacements, that are consistent with the geometric constraints of a body is set to zero to obtain the equations of motion. This principle is useful in deriving governing equations, boundary conditions and obtaining approximate solutions by virtual methods. Energy principles provide another means to obtain the governing equations and their solutions. In the present work, the principle of virtual work is used to derive the equations of motion for FG-CNT plates. The governing equations of higher-order theory for the displacement model given in Eq. (3) will be derived using the dynamic version of the principle of virtual displacements, i.e.

$$\int_0^T (\delta U + \delta V - \delta K)\, dt = 0 \qquad ...(6)$$

Where,

δU = Virtual strain energy i.e.,

$$\int_A \left\{ \int_{-h/2}^{h/2} \left[\sigma_x \delta\varepsilon_x + \sigma_y \delta\varepsilon_y + \tau_{xy}\delta\gamma_{xy} + \tau_{xz}\delta\gamma_{xz} + \tau_{yz}\delta\gamma_{yz}\right] dz \right\} dx\, dy$$

δV = Virtual work done by applied forces i.e.,

$$-\int q\delta w_0\, dx\, dy$$

δK = Virtual kinetic energy i.e.,

$$\int_A \{ \int_{-h/2}^{h/2} \rho_0 \left[\left(\dot{u}_0 + Z\dot{\theta}_x + Z^2\dot{u}_0^* + Z^3\dot{\theta}_x^*\right)\left(\delta\dot{u}_0 + Z\delta\dot{\theta}_x + Z^2\delta\dot{u}_0^* + Z^3\delta\dot{\theta}_x^*\right) + \left(\dot{v}_0 + Z\dot{\theta}_y + Z^2\dot{v}_0^* + Z^3\dot{\theta}_y^*\right)\left(\delta\dot{v}_0 + Z\delta\dot{\theta}_y + Z^2\delta\dot{v}_0^* + Z^3\delta\dot{\theta}_y^*\right) + \dot{w}_0\delta\dot{w}_0 \right] dz \}\, dx\, dy$$

$\delta U + \delta V$ = Total potential energy

where,

q = distributed load over the surface of the plate.

$\boldsymbol{\rho_0}$ = Density of plate material

On substituting for δU, δV and δK in to the virtual work statement in Eq. (6) and integrating through the thickness, integrating by parts and collecting the coefficients of each of virtual displacements $\delta u_o \delta v_0$, δw_0, $\delta\theta_x$, $\delta\theta_y$, δu_0^*, δv_0^*, $\delta\theta_x^*$, $\delta\theta_y^*$ in a domain of any differentiation the statement of virtual work is obtained as:

$$\delta u_0 : \frac{\partial N_x}{\partial x} + \frac{\partial N_{xy}}{\partial y} = I_1\ddot{u}_0 + I_2\ddot{\theta}_x + I_3\ddot{u}_0^* + I_4\ddot{\theta}_x^*$$

$$\delta v_0 : \frac{\partial N_y}{\partial y} + \frac{\partial N_{xy}}{\partial x} = I_1\ddot{v}_0 + I_2\ddot{\theta}_y + I_3\ddot{v}_0^* + I_4\ddot{\theta}_y^*$$

$$\delta w_0 : \frac{\partial Q_x}{\partial x} + \frac{\partial Q_y}{\partial y} + q = I_1\ddot{w}_0$$

$$\delta\theta_x : \frac{\partial M_x}{\partial x} + \frac{\partial M_{xy}}{\partial y} - Q_x = I_2\ddot{u}_0 + I_3\ddot{\theta}_x + I_4\ddot{u}_0^* + I_5\ddot{\theta}_x^*$$

$$\delta\theta_y : \frac{\partial M_y}{\partial y} + \frac{\partial M_{xy}}{\partial x} - Q_y = I_2\ddot{v}_0 + I_3\ddot{\theta}_y + I_4\ddot{v}_0^* + I_5\ddot{\theta}_y^*$$

$$\delta u_0^* : \frac{\partial N_x^*}{\partial x} + \frac{\partial N_{xy}^*}{\partial y} - 2S_x = I_3\ddot{u}_0 + I_4\ddot{\theta}_x + I_5\ddot{u}_0^* + I_6\ddot{\theta}_x^*$$

$$\delta v_0^* : \frac{\partial N_y^*}{\partial y} + \frac{\partial N_{xy}^*}{\partial x} - 2S_y = I_3\ddot{v}_0 + I_4\ddot{\theta}_y + I_5\ddot{v}_0^* + I_6\ddot{\theta}_y^*$$

$$\delta\theta_x^* : \frac{\partial M_x^*}{\partial x} + \frac{\partial M_{xy}^*}{\partial y} - 3Q_x^* = I_4\ddot{u}_0 + I_5\ddot{\theta}_x + I_6\ddot{u}_0^* + I_7\ddot{\theta}_x^*$$

$$\delta\theta_y^* : \frac{\partial M_y^*}{\partial y} + \frac{\partial M_{xy}^*}{\partial x} - 3Q_y^* = I_4\ddot{v}_0 + I_5\ddot{\theta}_y + I_6\ddot{v}_0^* + I_7\ddot{\theta}_y^* \quad \text{...(7)}$$

Where the in-plane force and moment resultants are defined as:

$$\begin{Bmatrix} N_x & | & N_x^* \\ N_y & | & N_y^* \\ N_{xy} & | & N_{xy}^* \end{Bmatrix} = \sum_{L=1}^{n} \int_{-h/2}^{h/2} \begin{Bmatrix} \sigma_x \\ \sigma_y \\ \tau_{xy} \end{Bmatrix} \left[1 \mid z^2\right] dz \quad \text{...(8)}$$

$$\begin{Bmatrix} M_x & | & M_x^* \\ M_y & | & M_y^* \\ M_{xy} & | & M_{xy}^* \end{Bmatrix} = \sum_{L=1}^{n} \int_{-h/2}^{h/2} \begin{Bmatrix} \sigma_x \\ \sigma_y \\ \tau_{xy} \end{Bmatrix} \left[Z \mid Z^3\right] dz \quad \text{...(9)}$$

Transverse force resultants and the inertias are given by:

$$\begin{Bmatrix} Q_x & | & S_x & | & Q_x^* \\ Q_y & | & S_y & | & Q_y^* \end{Bmatrix} = \sum_{L=1}^{n} \int_{-h/2}^{h/2} \begin{Bmatrix} \tau_{xz} \\ \tau_{yz} \end{Bmatrix} \left[1 \mid Z \mid Z^2\right] dz \quad \text{...(10)}$$

$$I_1, I_2, I_3, I_4, I_5, I_6, I_7 = \int_{-h/2}^{h/2} \rho_0 (1, z, z^2, z^3, z^4, z^5, z^6)\, dz \quad \text{...(11)}$$

where,

$$\rho_0 = V_{CNT}(z)\rho^{CNT} + V_m(z)\rho^m$$

The resultants in Equations (8)-(10) can be related to the total strains in Eq. (4) by the following matrix:

$$\begin{Bmatrix} N \\ N^* \\ -- \\ M \\ M^* \\ -- \\ Q \\ Q^* \end{Bmatrix} = \begin{bmatrix} A & B & 0 \\ B^t & D_b & 0 \\ 0 & 0 & D_s \end{bmatrix} \begin{Bmatrix} \varepsilon_0 \\ \varepsilon_0^* \\ -- \\ K \\ K^* \\ -- \\ \phi \\ \phi^* \end{Bmatrix} \quad ...(12)$$

Where,

$N = [N_x \;\; N_y \;\; N_{xy}]^t ; N^* = [N_x^* \;\; N_y^* \;\; N_{xy}^*]^t$

N, N^* are called the in-plane force resultants

$M = [M_x \;\; M_y \;\; M_{xy}]^t ; M^* = [M_x^* \;\; M_y^* \;\; M_{xy}^*]^t$

M, M^* are called as moment resultants

$Q = [Q_x \;\; Q_y]^t ; Q^* = [S_x \;\; S_y \;\; Q_x^* \;\; Q_y^*]^t$

Q, Q^* denotes the transverse force resultants and also

$\varepsilon_0 = [\varepsilon_{x0} \;\; \varepsilon_{y0} \;\; \varepsilon_{xy0}]^t ; \varepsilon_0^* = [\varepsilon_{x0}^* \;\; \varepsilon_{y0}^* \;\; \varepsilon_{xy0}^*]^t \; k = [k_x \;\; k_y \;\; k_{xy}]^t ; k^* = [k_x^* \;\; k_y^* \;\; k_{xy}^*]^t \quad \phi = [\phi_x \;\; \phi_y]^t ; \phi^* = [\varepsilon_{xz0} \;\; \varepsilon_{yz0} \;\; \phi_x^* \;\; \phi_y^*]^t$

The elements of matrices [A], [B], [D], and [Ds] are calculated using Eq. (5), and Eq. (8)-(10) using the effective properties of the respective FG-CNT plate from Eq. (2).

III. ANALYTICAL SOLUTIONS

Composite plates are generally classified by referring to the type of support used. The analytical solutions of the Eq. (7) - (12) for simply supported FG-CNT plates are dealt here. Assuming that the plate is simply supported in such a manner that normal displacement is admissible, but the tangential displacement is not, solution functions that completely satisfy the boundary conditions in the equations below are assumed as follows:

$$u_0(x,y) = \sum_{m=1}^{\infty}\sum_{n=1}^{\infty} U_{mn} \cos\alpha x \sin\beta y$$

$$v_0(x,y) = \sum_{m=1}^{\infty}\sum_{n=1}^{\infty} V_{mn} \sin\alpha x \cos\beta y$$

$$w_0(x,y) = \sum_{m=1}^{\infty}\sum_{n=1}^{\infty} W_{mn} \sin\alpha x \sin\beta y$$

$$\theta_x(x,y) = \sum_{m=1}^{\infty}\sum_{n=1}^{\infty} X_{mn} \cos\alpha x \sin\beta y$$

$$\theta_y(x,y) = \sum_{m=1}^{\infty}\sum_{n=1}^{\infty} Y_{mn} \sin\alpha x \cos\beta y$$

$$u_0^*(x,y) = \sum_{m=1}^{\infty}\sum_{n=1}^{\infty} U_{mn}^* \cos\alpha x \sin\beta y$$

$$v_o^*(x,y)=\sum_{m=1}^{\infty}\sum_{n=1}^{\infty}V_{mn}^*\sin\alpha x\cos\beta y$$

$$\theta_x^*(x,y)=\sum_{m=1}^{\infty}\sum_{n=1}^{\infty}X_{mn}^*\cos\alpha x\sin\beta y$$

$$\theta_y^*(x,y)=\sum_{m=1}^{\infty}\sum_{n=1}^{\infty}Y_{mn}^*\sin\alpha x\cos\beta y \quad ...(13)$$

for $\mathbf{0}\le \boldsymbol{x}\le \boldsymbol{a}\,;\mathbf{0}\le \boldsymbol{y}\le \boldsymbol{b}$

The mechanical load is expanded in double Fourier sine series as:

$$q(x,y)=\sum_{m=1}^{\infty}\sum_{n=1}^{\infty}Q_{mn}\sin\alpha x\sin\beta y \quad ...(14)$$

Where,

$$\alpha=\frac{m\pi}{a} \text{ and } \beta=\frac{n\pi}{b}$$

Substituting Eq. (13) into Eq. (7) and collecting the coefficients we obtain:

$$[[\boldsymbol{S}]_{9X9}-[\boldsymbol{M}]_{9X9}\omega^2]\begin{Bmatrix}\boldsymbol{U_{mn}}\\ \boldsymbol{V_{mn}}\\ \boldsymbol{W_{mn}}\\ \boldsymbol{X_{mn}}\\ \boldsymbol{Y_{mn}}\\ \boldsymbol{U_{mn}^*}\\ \boldsymbol{V_{mn}^*}\\ \boldsymbol{X_{mn}^*}\\ \boldsymbol{Y_{mn}^*}\end{Bmatrix}=\begin{Bmatrix}\mathbf{0}\\ \mathbf{0}\\ \mathbf{0}\\ \mathbf{0}\\ \mathbf{0}\\ \mathbf{0}\\ \mathbf{0}\\ \mathbf{0}\\ \mathbf{0}\end{Bmatrix} ..(15)$$

We may obtain the natural frequencies and vibration modes for the plate problem, by solving the eigen value equation $([S]-[M]\omega^2)X = 0$ where X are the modes of vibration associated with the natural frequencies defined as ω.

IV. RESULTS AND DISCUSSION

A. *Comparative Studies*

In this section, examples are presented and discussed to validate the accuracy of the present higher-order shear deformation theory in predicting the frequencies of a simply supported functionally graded CNT reinforced composite plates.The material properties of which are as follows:

$E^m = 70\ GPa\,,\rho^m = 2.7\frac{g}{cm^3},\vartheta^m = 0.34$

SWCNT (single-walled carbontubes) are taken as the reinforcements and its properties are:

$E_{11}^{CNT} = 5.6466\ TPa,\ E_{22}^{CNT} = 7.0800 TPa,$

$G_{12}^{CNT} = 1.9445\ TP,\ \upsilon_{12}^{CNT} = 0.1$ and $\rho^{CNT} = 1400\ kg/m^3$

The value of volume fraction of CNT i.e., V_{CNT}^* is taken as 0.11, and the corresponding CNT efficiency parameters are $\eta_1 = 0.149\ and\ \eta_2 = 0.934$. It is assumed that the effective shear moduli $G_{13} = G_{23} = G_{12}\ and\ \eta_3 = \eta_2$.

Table 1: Non dimensional Fundamental Frequency of FG-CNT composite for uniform distribution subjected to sinusoidal loading

a/h values	V = 0.11	V = 0.14	V = 0.17
5	0.240742	0.250640	0.299307
10	0.067167	0.070113	0.083075

20	0.017381	0.018264	0.021210
50	0.002828	0.002945	0.003417
100	0.000589	0.000589	0.000589

Table2: Non dimensional Fundamental Frequency of FG-CNT composite for uniform distribution subjected to sinusoidal loading

a/h values	V = 0.11	V = 0.14	V = 0.17
5	0.251347	0.263838	0.315804
10	0.070702	0.074826	0.088967
20	0.014435	0.019443	0.022978
50	0.003142	0.003181	0.003708
100	0.000589	0.000589	0.001178

Presently computed results for different values of volume fraction and side-to-thickness ratios (a/h) are compared with those of B. Sidda Reddy[12].For convenience, natural frequency has been non dimensional zed as $=\omega h\sqrt{\rho_m/E_m}$

Table 3: non dimensional natural frequencies of a simply supported square Al/ZrO2 FG thick plate with m = 1 and n = 1 and different values of side-to-thickness ratios (a/h)

a/h	present	B.siddaredy[12]	Qian et al.[16]	Exact[17]
5	0.24078	0.2285	0.2152	0.2192
10	0.06716	0.0619	0.0584	0.0596
20	0.01738	0.0158	0.0149	0.0153

Table 1 represents the non dimensional fundamental frequencies of Al FG CNT using the formula above.

Table 3 shows the non dimensional natural frequencies of Al/ZrO2 FG thick plate. the present results are compared with the Al/ZrO2 previous results and it can be observed that the inclusion of CNT as reinforcement improves the vibration behavior of the material.

B. Parametric Study

1) . Effect of Side-to-Thickness Ratio : ariation of non-dimensionalized natural frequencies for various side to thickness ratios $\left(\frac{a}{h}\right)$and for different volume fraction of CNT (V_{CNT}^{*}) for the displacement model are shown in Figures 2 - 6 for two different distributions (UD and FGX) of CNT. It is noticed that the volume fraction of CNT has little effect on natural frequencies as the side-to-thickness ratio increases.

ISSN: 2321-9653; IC Value: 45.98; SJ Impact Factor:6.887
Volume 5 Issue XI November 2017- Available at www.ijraset.com

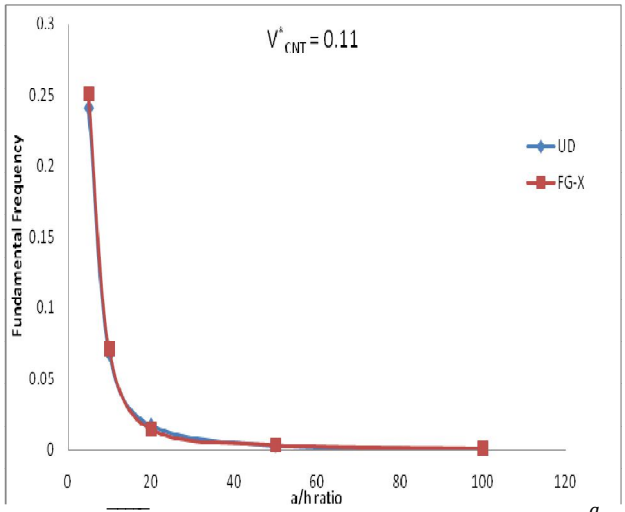

Figure 4.1 Non-dimensionalized frequencies $(\overline{w})$ as a function of side-to-thickness ratio $(\frac{a}{h})$ of an UD-CNT and FG-X plate for volume fraction of CNT 0.11

The above plot shows the variation of fundamental frequency for different aspect ratios for volume fraction 0.11. The aspect ratios are taken on the x-axis and the fundamental frequencies are taken on the y-axis. It is observed that as the aspect ratio increases, the fundamental frequencies decreases mas shown both for uniform and FG X distributions. The FG X distribution has slightly higher fundamental frequency when compared to the uniform distribution.

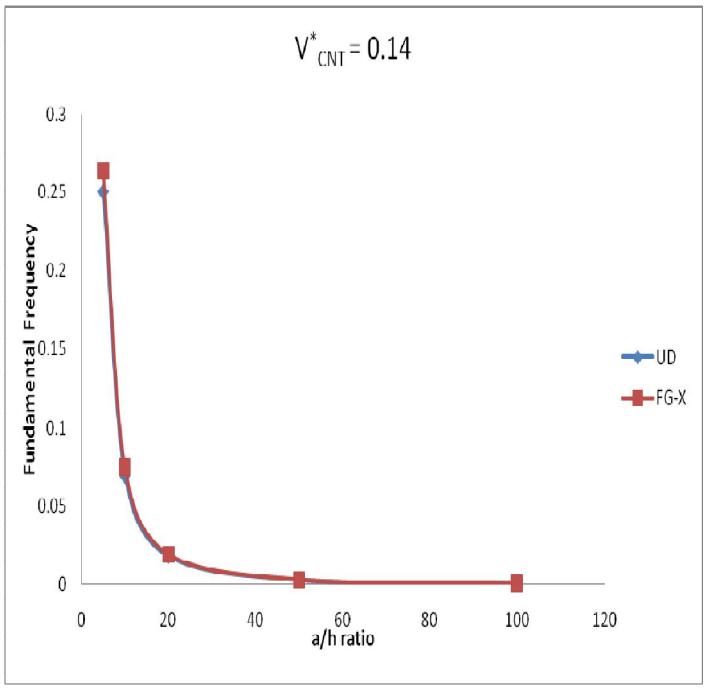

Figure 4.2. Non-dimensionalized frequency $(\overline{\square})$ as a function of side-to-thickness ratio $(\frac{\square}{h})$ of an UG CNT and FGX-CNT plate for volume fraction of CNT 0.14

The above plot shows the variation of fundamental frequency for different aspect ratios for volume fraction 0.14. The aspect ratios are taken on the x-axis and uthe fundamental frequencies are taken on the y-axis. It is observed that as the aspect ratio increases,the fundamental frequencies decreases mas shown both for uniform and FG X distributions. The FG X distribution has slightly higher fundamental frequency when compared to the uniform distribution.

ISSN: 2321-9653; IC Value: 45.98; SJ Impact Factor:6.887
Volume 5 Issue XI November 2017- Available at www.ijraset.com

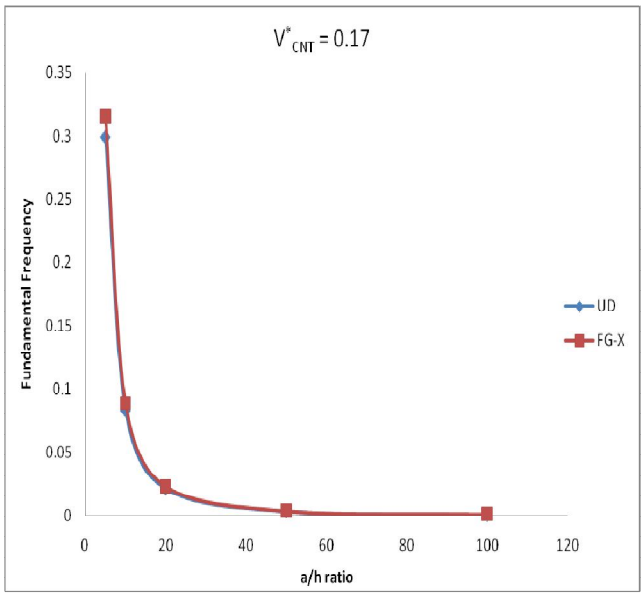

Figure 4.3 Non-dimensionalized frequencies as a function of side-to-thickness ratio ($\frac{\square}{h}$) of an UD-CNT and FG-X plate for different volume fraction of CNT.

The above plot shows the variation of fundamental frequency for different aspect ratios for volume fraction 0.11. The aspect ratios are taken on the x-axis and the fundamental frequencies are taken on the y-axis. It is observed that as the aspect ratio increases,the fundamental frequencies decreases as shown both for uniform and FG X distributions. The FG X distribution has slightly higher fundamental frequency when compared to the uniform distribution.

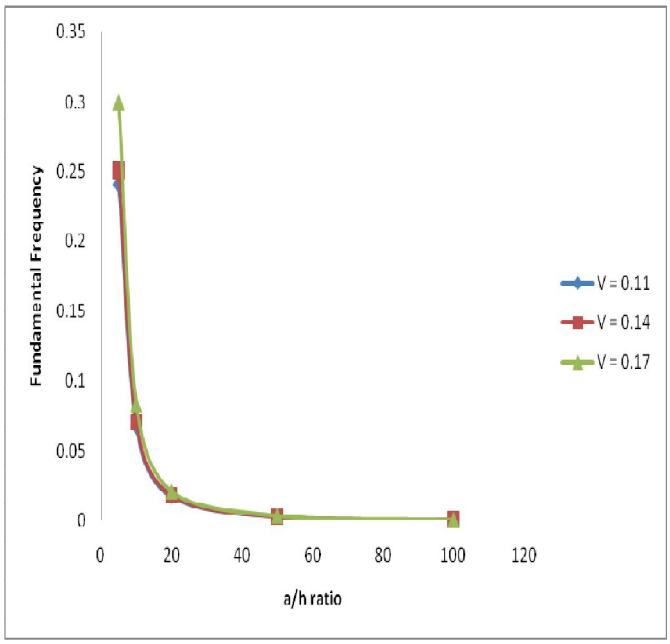

Figure 4.4 Non-dimensionalized frequencies as a function of side-to-thickness ratio ($\frac{\square}{h}$) of an UD-CNT plate for different volume fraction of CNT.

The above plot shows the variation of fundamental frequency for different aspect ratios for different volume fraction. The aspect ratios are taken on the x-axis and the fundamental frequencies are taken on the y-axis. It is observed that as the aspect ratio increases, the fundamental frequencies decreases mas shown both for uniform and FG X distributions. The FG X distribution has

slightly higher fundamental frequency when compared to the uniform distribution. As the volume fraction of the CNT increases there is very slight increase in the fundamental frequency of the material.

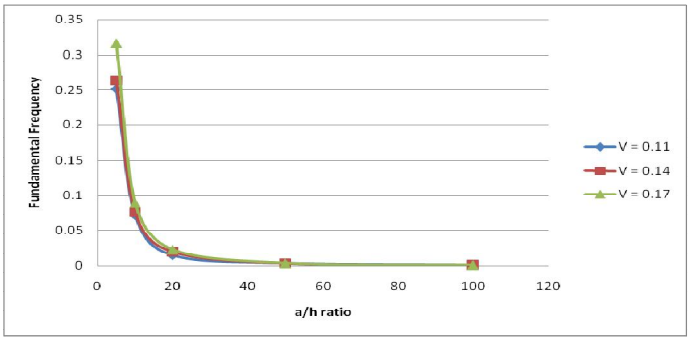

Figure 4.5 Non-dimensionalized frequencies as a function of side-to-thickness ratio ($\frac{a}{h}$) of an FG-X CNT plate for different volume fraction of CNT.

V. CONCLUSIONS

A higher-order shear deformation theory was employed for static bending behavior of simply supported functionally graded CNT reinforced composite plates without enforcing zero transverse shear stresses on the top and bottom surfaces of the plate. This eliminates the requirement of shear correction factors. The governing equations and boundary conditions are derived by utilizing the principle of virtual work. The governing equations are solved using Navier's type closed form solution, for FG-CNT plates subjected to sinusoidal load. Comparative studies are carried out to signify the accuracy and efficiency of the present theory. The gradation of material properties in the thickness direction can eliminate interface problems. The analytical formulations and solutions developed herein should be helpful in future studies in the design of FG-CNT plates for advanced technical applications. Also, the present research will be a useful benchmark for evaluating the other future plate theories and numerical methods, such as the finite element and mesh less methods. In conclusion it can be said that replacing zro2 with cnt in aluminium matrix improves vibration characteristics of the material.

REFERENCES

[1] Yamanouchi M., Hirai T., Shiota I., "Proceedings of First International Symposium on Functionally Gradient Materials", FGM Forum, Tokyo, 1990, Japan.
[2] Reddy, J.: Mechanics of laminated composite plates and shells. CRC Press, (2004)
[3] Phan, N.D.; Reddy, J.N.: Analysis of laminated composite plates using a higher-order shear deformation theory. Int. J. Numer. Methods Eng. **21**, 2201–2219 (1985).
[4] Esawi, A.M.K.K.; Farag, M.M.: Carbon nanotube reinforced composites: potential and current challenges. Mater. Des. **28**, 2394–2401 (2007).
[5] M. S. EL-Wazery, A. R. EL-Desouky, "A review on Functionally Graded Ceramic-Metal Materials", Environ. Sci. 6 (5) (2015) 1369-1376.
[6] M.H. Yas, N. Samadi, Free vibrations and buckling analysis of carbon nanotube-reinforcedcomposite Timoshenko beams on elastic foundation, International Journal of Pressure Vesselsand Piping., Vol. 98, pp.119-128, 2012.
[7] Huu-Tai Thai and ThucP.Vo, "A new sinusoidal shear deformation theory for bending, buckling, and vibration of functionally graded paltes". Appl Math Model,Vol. **37 (**2013) 3269-3281.
[8] J.N. Reddy and C.D. Chin, "Thermomechanical analysis of functionally graded cylinders and plates". J Therm stress, Vol. 21(1998) No.6, 593-626.
[9] T. Kant, and K. Swaminathan, "Analytical solutions for the static analysis of laminated composite and sandwich plates based on higher order refined theory". Composite struct, Vol. 56 (2002) No. 4, 329-344.
[10] T. Kant, and K. Swaminathan, "Analytical solutions for free vibration analysis of laminated composite and sandwich plates based on higher order refined theory". compositestruct, Vol. 53 (2001) No. 1, 73-85.
[11] W. Zhang et al. "the vibration analysis of FG-CNT reinforced composite plates subjected to in-plane loads based on State-space Levy method",
[12] Mohammad Rahim Nami "the free vibration of thick functionally graded carbon nanotube-reinforced rectangular composite plates based on three dimensional elasticity theory via differential quadrature method".
[13] Zhu J, Yang J and Kitipornchai S 2013 Dispersion spectrum in a functionally graded carbon nanotube-reinforced plate based on first-order shear deformation plate theory Compos. Part B 53 274-283
[14] T.Kant and K.Swaminathan "the natural frequency analysis of simply supported composite and sandwich plates using higher order shear deformation theory", Composites: Part B, Vol. 36, pp. 68_72(2005).
[15] Qiana, L. F., Batrab, R. C. and Chena, L. M., "Static and Dynamic Deformations of Thick Functionally Graded Elastic Plates by Using Higher-Order Shear and Normal Deformable Plate Theory and Meshless Local Petrov-Galerkin Method," Composites: Part B, Vol. 35, pp. 685_697 (2004).
[16] Vel, S. S. and Batra, R. C., "Three-Dimensional Exact Solution for the Vibration of Functionally Graded Rectangular Plates," Journal of Sound and Vibration, Vol. 272, pp. 703_730 (2004).

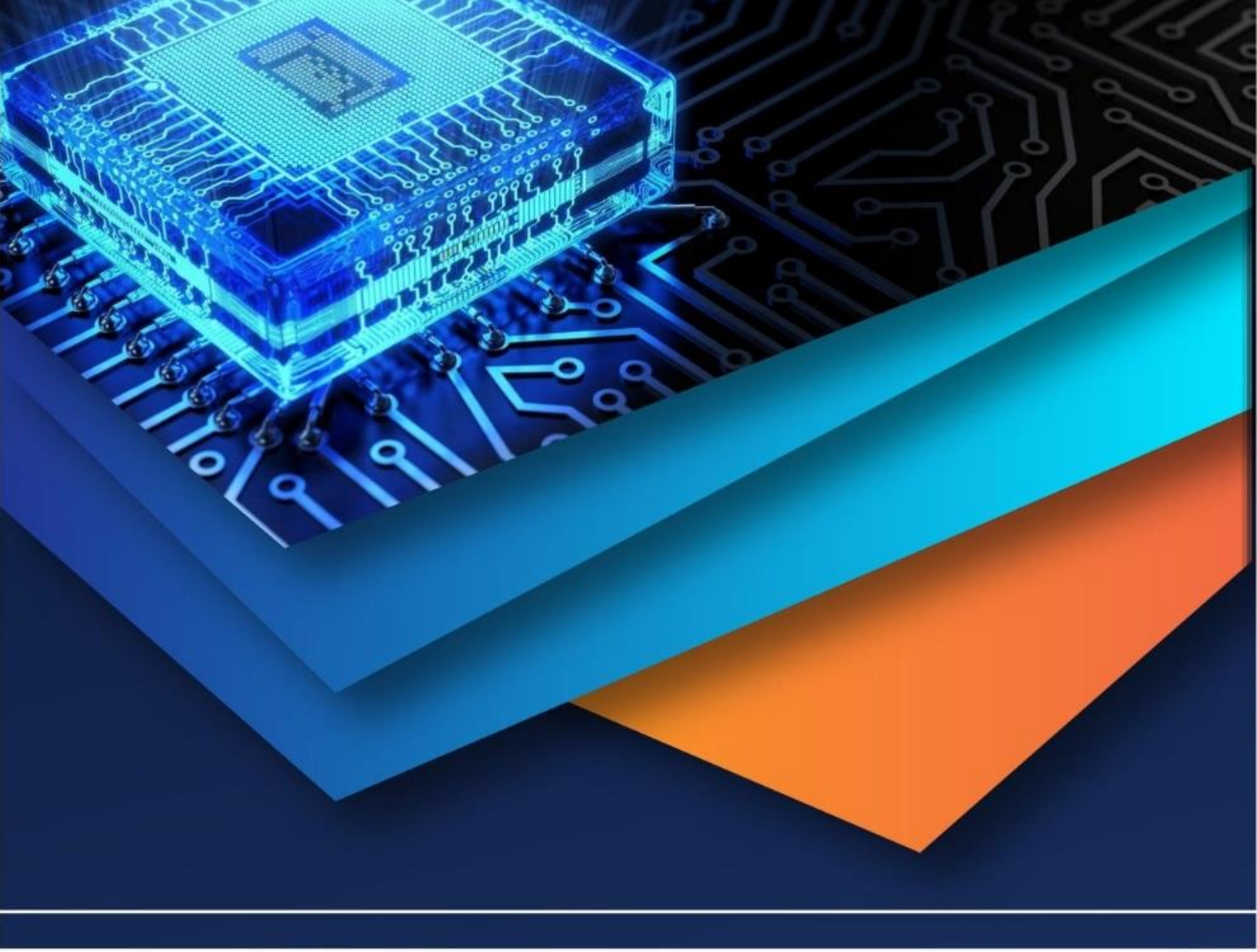

10.22214/IJRASET

45.98

IMPACT FACTOR: 7.129

IMPACT FACTOR: 7.429

INTERNATIONAL JOURNAL FOR RESEARCH

IN APPLIED SCIENCE & ENGINEERING TECHNOLOGY